INDIAN JOURNAL OF SCIENCE AND TECHNOLOGY

RESEARCH ARTICLE

OPEN ACCESS

Received: 26-10-2024

Accepted: 23-12-2024

Published: 12-02-2025

Citation: Dangi R, Redhu P, Kumari V (2025) Traffic Jerk Effect From Non-motor Automobiles and Velocity Prediction Effect in Car-Following Model Under V2X Environment. Indian Journal of Science and Technology 18(3): 258-267. https://doi.org/10.17485/IJST/v18i4.3517

* **Corresponding author**.

Poonamr.maths@mdurohtak.ac.in

Funding: None

Competing Interests: None

Published By Indian Society for Education and Environment (iSee)

ISSN
Print: 0974-6846
Electronic: 0974-5645

Traffic Jerk Effect From Non-motor Automobiles and Velocity Prediction Effect in Car-Following Model Under V2X Environment

Raveena Dangi[1], Poonam Redhu[1]*, Vijeta Kumari[1]

1 Department of Mathematics, MD University, Rohtak, 124001, Haryana, India

Abstract

Objectives: To enhance traffic flow stability and alleviate congestion, a car-following model that incorporates velocity prediction and traffic jerk is developed. **Methods:** A car-following model that considers the traffic jerk impact and velocity prediction is presented. The impact of the model on traffic stability and congestion is assessed using linear stability analysis in conjunction with the reductive perturbation technique for deriving mKdV equation and nonlinear calculations. Numerical simulations under periodic boundary conditions are used to validate theoretical results further. **Findings:** Using linear stability analysis, it is demonstrated that velocity prediction significantly expands the stable region of the phase diagram as compared to the optimal velocity model, whereas jerk behavior expands the unstable region. A "modified Korteweg-de Vries" equation (mKdV) is implemented to identify areas where congestion is most severe, indicating heavy traffic near the critical point. Based on nonlinear calculations, it has been demonstrated that traffic jerk effects from non-motor automobiles enlarge unstable regions on phase diagrams, while velocity prediction enlarges stable regions. Traffic flow is improved by this combination strategy, particularly in locations close to the main bottleneck point. Given that drivers are better equipped to modify their conduct in response to traffic circumstances, the results imply that drivers' behavior toward non-motor vehicles has a differential effect that directly reduces traffic congestion. The model's relevance to actual traffic situations is further supported by numerical simulations, which are applied using periodic boundary parameters that validate these theoretical solutions' practical efficacy. **Novelty:** The model integrates traffic jerk effect and velocity prediction, expanding traffic stability and mitigating congestion more effectively than existing models.

Keywords: Traffic flow; Traffic jerk; Velocity prediction; Simulation; Car-following model

1 Introduction

Increased air pollution and traffic congestion brought on by the rise in automobile ownership as a result of urbanization and economic expansion have made the development of intelligent transportation system technologies necessary. In order to prevent traffic bottlenecks, limit collisions, save energy, and lower emissions, researchers are trying to enhance the precision of traffic flow probabilities. Theories like artificial neural networks, deep learning, fuzzy logic, lattice hydrodynamics, vehicle-infrastructure communication, and vehicle diversity have all been used to create different traffic flow models[1–9]. A crucial component of ITS technology, vehicle-to-everything (V2X) provides a practical way to ease traffic and enhance road safety[10–12]. V2X enhances driver-vehicle cooperation by enabling communication between cars and the environment[13–16]. This modern technology is the paramount choice for relieving the growing issues with our present transportation system as it has effectively raised road safety and lowered traffic congestion. According to the literature, most researchers have ignored the driver's supervision of beginning wave in a V2X setting in favor of concentrating on how CF models affect traffic flow features. Better methods for enhancing road safety have been made possible by improvements in driving behavior modeling, which have made it possible to forecast possible collisions with greater accuracy. In addition to assessing and determining the driving behavior of the cars in front of them, drivers manage traffic. To enable drivers to respond appropriately, it is crucial to have a forecast time before the car ahead of them begins moving. There are several real-world uses for investigating traffic bifurcation, including regulating traffic flow, developing traffic simulators, and comprehending traffic behavior. Vehicles frequently experience abrupt changes in speed in real-world traffic situations; this phenomenon is known as traffic jerk. Phantom traffic bottlenecks are caused by this type of disruption, which spreads quickly upstream in traffic. Numerous researchers have examined various traffic flow models taking traffic jerk into account in recent years. By considering the traffic jerk effect, Redhu and Siwach[17] presented the expanded flux difference lattice hydrodynamics model. Linear and nonlinear stability outputs were used to assess the effect of jerk parameter. Zhai and Wu[18] presented a continuum traffic model that considered the effects of driver qualifications and traffic jerks. The outcome of their simulations indicated that both jerk and driver characteristics had a major impact on emissions and flow stability. A macro traffic flow model was put forward by Cheng et al.[19]. It took into account both anticipation and traffic jerk at the same time. Yi et al.[20] give an enhanced "car-following model" that takes the effect of non-motor vehicles and traffic jerks into consideration. The outcomes of the analytical and numerical analyses demonstrated that the enhanced model could accurately depict the phase transition and critical events under actual tracing settings. In order to interrogate the effects of driver memory and jerk on traffic flow, Jin et al.[21] designed an enhanced car-following model. Following that, the evolution of traffic crowdedness and the associated energy use were examined. It makes sense to draw conclusions from the traffic jerk that has a major effect on traffic flow stability and must be taken into account when modeling car-following behavior. Drivers are finding it increasingly difficult to make fast choices in traffic systems. Making educated judgments when traveling requires knowing a vehicle's speed and the number of other cars on the road close to it. Drivers look for advanced insights on the anticipated future state of the ongoing vehicle to prevent traffic accidents and congestion[22]. By having access to predicted data, drivers may pick an ideal route and time to avoid crowded areas by anticipating future traffic conditions[23]. Recently, Yadav[24] has introduced a vehicle-following model that accounts for the impact of low visibility on drivers' perception and response times and the adjustment of traffic jerk dynamics in inclement weather.

In addition to benefiting individual drivers, it also lessens traffic, which saves time for all users of the road. In order to enable the tailing vehicle to modify its ongoing speed in order to reach the desired velocity, we proposed a car-following model in this paper that takes into consideration the idea of receiving advanced information relating to the anticipated future condition of the leading vehicle in terms of velocity. Predicting how cars will behave and travel in the future is a challenging and time-consuming process. The goal of this study is to investigate how V2X settings, which provide info on the speed and distance of cars ahead, might affect the stability of traffic flow. Furthermore, the model could make it easier to correctly forecast how front-end vehicles would behave, enabling drivers to anticipate their motions and react appropriately. The study's findings will offer insightful information for enhancing road traffic movement and safety.

The proposed model enhances traffic stability by integrating velocity prediction, which expands the stable regions of traffic dynamics, and incorporating traffic jerk effects, which realistically capture destabilizing factors. This combination allows for better modeling of driver responses to traffic conditions and supports targeted interventions to mitigate congestion.

The paper's layout is provided below. A new CF model is created in Section 2 to forecast vehicle speeds and the traffic jerk effect. In Section 3, the theoretical analysis is confirmed by numerical simulation, linear analysis, and the derivation of the "mKdV equation" using nonlinear analysis to validate the efficiency of the suggested model and discussion. Lastly, a brief overview of the conclusion, containing significant concepts and findings, is given in Section 4.

2 Methodology

This section provides an introduction to the "optimal velocity model" and then presents the different models that describe the traffic jerk and velocity prediction effect.

2.1 Modelling

The OV model, which was first presented by Bando et al. in 1995, is based on the difference between the driver's anticipated and actual vehicle speeds. The following is the equation that represents this model:

$$\frac{dv_n}{dt} = \alpha[V(\triangle x_n(t) - v_n(t)] \tag{1}$$

In this equation, α represents sensitivity of the driver, while x_n and v_n represent the vehicle's location and velocity, respectively, '$\Delta x_n = x_{n+1} - x_n$' is the distance between vehicles $n+1$ and n and $V(\Delta x_n)$ is the optimal velocity of the vehicle n. Furthermore, based on the "Optimal Velocity Model" (OVM), the proposed "Full Velocity Difference Model" (FVDM) is as follows:

$$\frac{dv_n}{dt} = \alpha[V(\triangle x_n(t) - v_n(t))] + \lambda \Delta v_n(t) \tag{2}$$

where α the sensitivity of the velocity is different and $\Delta v_n = v_{n+1} - v_n$ is the difference in velocity between successive vehicles.

Driving is affected by the non-motor vehicles on the road. As long as the car in front continues to drive in front of it, the driver of the vehicle behind it will also follow it. Simultaneously, the driver will analyze how jerks might affect vehicle control. To mitigate the impact of speed changes, drivers may modify their driving speed when the jerk is high to make it difficult to manage the car. As vehicles are more, the anticipated perception of flow by the following driver will decrease correspondingly. In conclusion, the relationship between velocity prediction and traffic jerk is essential for improving vehicle control, understanding and simulating dynamic traffic behavior, and streamlining traffic. Jerk offers an extra level of information that improves velocity change prediction, resulting in more precise traffic models. Consequently, a novel car-following model has been developed to account for the impact of traffic jerk with the prediction of velocity of n+1 vehicle on driving. The governing equation is outlined below:

$$\frac{dv_n}{dt} = \alpha\left[V(\triangle x_n(t+\tau_p)) - v_n(t)\right] + k[v_{n+1}(t+\tau_p) - v_{n+1}(t)\Big] + \beta[v_n(t) - v_n(t-\tau_r)] \tag{3}$$

Here $v_{n+1}(t+\tau_p) - v_{n+1}(t)$ denotes the difference of velocity of the future and present velocity of the prior vehicle n+1; k is response coefficient of the prevision of velocity and τ_p is driver prediction time. β is the traffic-jerk coefficient that corresponds to non-motor vehicle motion. The temporal dynamics of the vehicle flow are represented by the jerk parameter profile and more non-motor vehicles on the road often result in traffic congestion and flow instability. Furthermore, $v_n(t) - v_n(t-\tau_r)$ shows the jerking behavior of the nth vehicle at time t with time delayed τ_r.

For simplification, we can rewrite Equation (3) as follows:

$$\frac{d^2x_n}{dt^2} = \alpha\left[V(\Delta x_n(t+\tau_p)) - \frac{dx_n(t)}{dt}\right] + k\left[\frac{dx_{n+1}(t+\tau_p)}{dt} - \frac{dx_{n+1}(t)}{dt}\right] + \beta\left[\frac{dx_n(t)}{dt} - \frac{dx_n(t-\tau_r)}{dt}\right] \tag{4}$$

Using Taylor series expansion, we can write

$$V(\Delta x_n(t+\tau_p)) = V(\triangle x_n(t)) + \tau_p V'(\Delta x_n(t))\frac{d\Delta x_n(t)}{dt} + \frac{\tau_p^2 V''(\Delta x_n(t))}{2}\frac{d^2\Delta x_n(t)}{dt^2} + \dots \tag{5}$$

and

$$v_n(t+\tau_p) = v_n(t) + \tau_p v_n'(t) \tag{6}$$

Using Equations (5) and (6) in Equation (4), we get

$$\begin{aligned}\frac{d^2x_n(t)}{dt^2} = \alpha\Bigg[&V(\triangle x_n(t)) + \tau_p V'(\Delta x_n(t))\frac{d\Delta x_n(t)}{dt} + \frac{\tau_p^2 V''(\Delta x_n(t))}{2}\frac{d^2\Delta x_n(t)}{dt^2} - \frac{dx_n(t)}{dt}\Bigg] + \\ &k\frac{\tau_p}{\tau}\left[\frac{dx_{n+1}(t)}{dt} - \frac{dx_{n+1}(t-\tau)}{dt}\right] + \frac{\beta\tau_r}{\tau}\left[\frac{dx_n(t)}{dt} - \frac{dx_n(t-\tau)}{dt}\right]\end{aligned} \tag{7}$$

3 Results and D iscussion

3.1 Linear Stability An alysis

The traffic flow is significantly affected by information about nearby vehicles. However, little work has been done to examine how traffic jerk affects traffic flow from a linear stability analysis aspect. In this phase, we derive stability conditions using a linear stability theory of our proposed model. The state of uniform flow of traffic is when all vehicles flow at ideal speed and constant headway. By assuming $x_n(t) = x_n^{(0)}(t) + y_n(t)$, where '$x_n^{(0)}(t) = hn + V(h)t$' and $y_n(t)$ is a little deviation as to the steady state, so Equation (7) can be reimported as

$$\frac{d^2 y_n(t)}{dt^2} = \alpha\left[V^{'}(h)\Delta y_n(t) + \tau_p V^{'}\frac{dy_n(t)}{dt} + \frac{\tau_p^2 V^{''}}{2}\frac{d^2 y_n(t)}{dt^2} - \frac{dy_n(t)}{dt}\right] + k\frac{\tau_p}{\tau}\left[\frac{dy_{n+1}(t)}{dt} - \frac{dy_{n+1}(t-\tau)}{dt}\right] + \frac{\beta\tau_r}{\tau}\left[\frac{dy_n(t)}{dt} - \frac{dy_n(t-\tau)}{dt}\right] \tag{8}$$

After using $y_n(t) = e^{ijk+zt}$ in Equation (5), we get

$$z^2 = \alpha\left[V^{'}(h)\left(e^{ik}-1\right) + \tau_p V^{'} z + \frac{\tau_p^2 V^{''} z}{2} - z\right] + \frac{k\tau_p}{\tau}\left[ze^{ik}\left(1-e^{-\tau z}\right)\right] - \frac{\beta\tau_p}{\tau}\left[z - ze^{-\tau z}\right] \tag{9}$$

After replacing $z = z_1(ik) + z_2(ik)^2 + \ldots$ in Equation (7) and we can find the coefficients of (ik) and $(ik)^2$ from the expression of z, we get

$$z_1 = V'(h)(1+\tau_p) \tag{10}$$

$$z_2 = \frac{(V^{'}(h))^2\left[k\tau_p - \beta\tau_r - 1\right]}{\alpha} + \frac{V^{'}(h)}{2} + \tau_p v^{'}(h) \tag{11}$$

If z_2 is negative, the uniformly steady-state flow exhibits instability and if z_2 is positive, the uniform flow becomes stable according to the long wavelength modes. Therefore, the neutral stability curve occurs when z_2> 0. So, it holds if

$$\alpha > \frac{-2V^{'}(h)\left[k\tau_p - \beta\tau_r - 1\right]}{1+2\tau_p} \tag{12}$$

Therefore, the neutral stability curve is obtained if

$$\alpha = \frac{-2V^{'}(h)\left[k\tau_p - \beta\tau_r - 1\right]}{1+2\tau_p} \tag{13}$$

Equation (13) suggests that traffic flow stability is significantly impacted equally by the traffic jerk effect and the velocity prediction of vehicles. While keeping the parameters $\beta = 0,\ \tau_p = 0,\ \tau_r = 0\ and\ k = 0$, then the stability condition inEquation (13) bears similarity to the optimal velocity model's condition. Furthermore, if we take $k = 0.2,\ \tau_r = 0.2,\ \tau_p = 0.2\ and\ \beta = 0.2$, Figure 1 (**a**) shows the notable matches between the OVM and the new suggested model. A clearer, more stable zone can be seen when comparing the OVM and new model findings. The suggested model represents a more stable zone than the OV model; it is clearly an improvement over the literature currently in publication and contributes to the improvement of vehicle stability during movement processes. It signifies the role of non-motor vehicles in traffic flow with a predictive velocity of prior vehicles.

Figure 1 (**b**) depicts that when predictive time τ_p, jerk coefficients β and the delay time τ_r are fixed and the coefficient of velocity prediction 'k' varies from a low value to a high value, then the apex of the stable region falls down and in Figure 1 (**c**), unstable region decreases with the increase in the value of τ_p, so we can say that Figure 1 (**b**) and Figure 1 (**c**) depict the dependence of the stability of the proposed model on the predictive information of the velocity of the vehicles in front of moving vehicles. It is clear that the traffic flow is more stable if the vehicle gets information about the ahead. Figure 1 (**d**) illustrates that the stability of the proposed model decreases when the jerk coefficient β increases due to increased traffic flux. These results imply that there may be an opportunity to enhance traffic stability and lessen congestion if the feedback coefficient concentrates more on the predictive information of the vehicle's velocity. In brief, the value of predictive time τ_p, jerk coefficients β, velocity prediction coefficient k and the delay time τ_r play a significant role in traffic flow outcomes. These findings are in line with actual traffic occurrences.

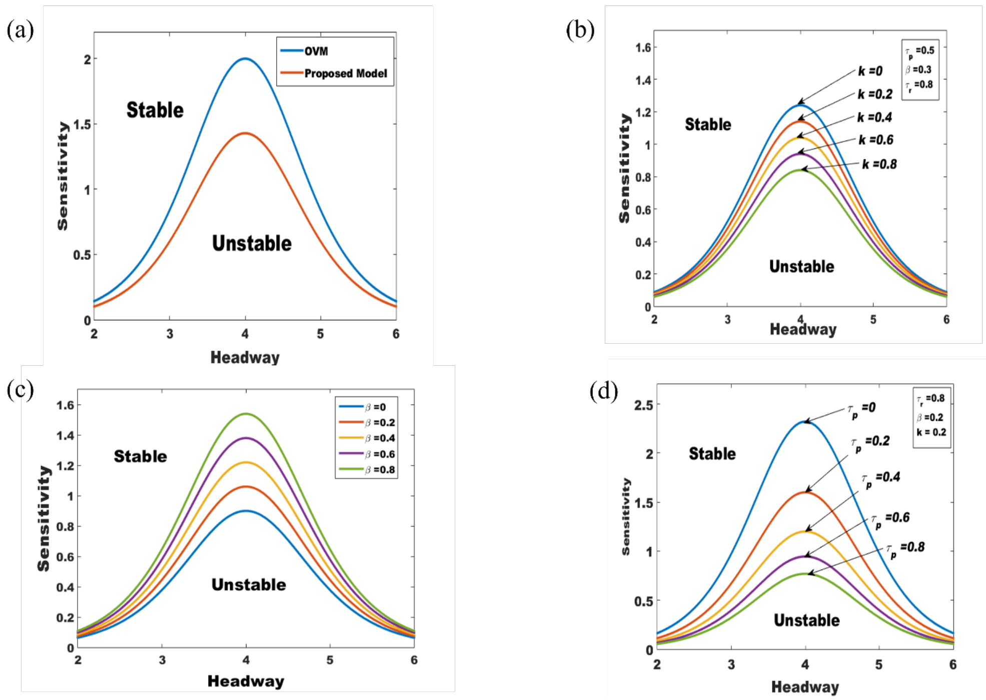

Fig 1. (a) Comparison between OVM and proposed model (b) $\beta = \mathbf{0.3}$, $\tau_{\mathbf{p}} = \mathbf{0.5}$, $\tau_{\mathbf{r}} = \mathbf{0.8}$ **and k vary from 0 to 0.8 (c)** $\tau_{\mathbf{r}} = \mathbf{0.8}$, $k = \mathbf{0.2}$, $\tau_{\mathbf{p}} = \mathbf{0.5}$ **and** β **vary from 0 to 0.8 (d)** $\beta = \mathbf{0.2}$,$\tau_{\mathbf{r}} = \mathbf{0.8}$, $k = \mathbf{0.2}$ **and** $\tau_{\mathbf{p}}$ **vary from 0 to 0.8.**

3.2 Nonlinear Stability Analysis

Here, we intend to analyse the "nonlinear stability" of the framed model by using the reductive perturbation method. The nonlinear stability analysis, through the derivation of the mKdV equation, provides critical insights into the dynamics of traffic congestion near the critical point. These theoretical findings are corroborated by the numerical simulations, which demonstrate similar congestion patterns and validate the practical relevance of the model. Therefore, we introduce the slow scale variables j for space and t for time variable. The correlative slow variables 'X' and 'T' are as follows:

$$X = \varepsilon\,(j + bt)\,,\ \ T = \varepsilon^3 t \tag{14}$$

where "b" is unknown to be calculated. By correlating to these slow-scale variables X and T, we can explore the response of the model to small perturbations while operating close to its critical point. Equation (4) can be written in the form of headway as follows:

$$\begin{aligned}\frac{d^2\Delta x_n}{dt^2} = \alpha\left[V\left(\Delta x_{n+1}\left(t+\tau_p\right)\right) - V\left(\Delta x_n\left(t+\tau_p\right)\right) - \frac{dx_n\left(t\right)}{dt}\right] + \\ k\left[\frac{d\Delta x_{n+1}\left(t+\tau_p\right)}{dt} - \frac{d\Delta x_{n+1}\left(t\right)}{dt}\right] + \beta\left[\frac{d\Delta x_n\left(t\right)}{dt} - \frac{d\Delta x_n\left(t-\tau_r\right)}{dt}\right]\end{aligned} \tag{15}$$

By defining headway as

$$\Delta x_n\left(t\right) = h_c + \epsilon R(X,T) \tag{16}$$

Using Equations (14) and (16) in Equation (15), and after expanding upto 5$^{\text{th}}$ order of ϵ, we get

$$\epsilon^2 g_1 \partial_X R + \epsilon^3 g_2 \partial_X^2 R + \epsilon^4 (g_3 \partial_X^3 R + g_4 \partial_X R^3 - \partial_T R) + \epsilon^5 (g_5 \partial_X^4 R + g_6 \partial_X^2 R^3 + g_7 \partial_X \partial_T R) = 0\& \tag{17}$$

The coefficients $g_i' s$ are given in the Table 1, where

$$V' = V'(h_c) = \frac{dV(\triangle x_n)}{d\triangle x_n}\bigg|\ \triangle x_n = h_c\ , V''' = V'''(h_c) = \frac{d_3 V(\triangle x_n)}{d\triangle x^3{}_n}\bigg|\ \ \triangle x_n = h_c \tag{18}$$

Near the critical point $(h_c,\ \alpha_c)$, we consider the neighborhood of the α_c as

$$\frac{\alpha_c}{\alpha} = (1+\epsilon^2\ ) \tag{19}$$

Assuming, $b = V'(h)$ and eliminating the 2nd and 3rd order terms of ϵ, we get

$$\epsilon^4(\partial_T R - k_1\partial_X^3 R + k_2\partial_X R^3) + \epsilon^5(k_3\partial_X^2 R + k_4\partial_X^4 R + k_5\partial_X^2 R^3) = 0 \tag{20}$$

The values of $k_i's$ are given in the Table 2.

Equation (17) can be converted into a standard "mKdV equation", by using the following transformations:

Table 1. Values of g_i^s

g_1	$V^{'}(h) - b$	$g_2 =$	$\frac{V^{'}(h)(1+2b\tau_p)}{2} - \frac{b^2\tau}{2} + \tau k b^2\tau_p - \tau b^2\tau_r\beta$
g_3	$\frac{V^{'}(h)(1+3b\tau_p+3b^2\tau_p^2)}{6} - \frac{b^3\tau^2}{6} + \frac{\tau k}{2}\left(b^3\tau_p^2 + \tau\tau_p b^3 + 2b^2\tau_p\right) - \frac{\tau\beta b^3}{2}(\tau\tau_r - \tau_r^2)$		
g_4	$\frac{V^{'''}(h)}{6}$		
g_5	$\frac{V^{'}(h)}{24}(1+6b^2\tau_p^2+4b^3\tau_p^3+4b\tau_p) - \frac{b^4\tau^3}{24} + \frac{\tau k}{24}(b^4\left(6\tau\tau_p^2+4\tau_p{}^3+4\tau^2\tau_p\right) + \frac{b^2\tau_p}{2} + \frac{b^3}{2}\left(\tau\tau_p+\tau_p^3\right) - \frac{\tau\beta b^4}{24}(-6\tau\tau_r^2 + 4\tau_r^3 + 4\tau^2\tau_r)$		
g_6	$\frac{V^{'''}(h)}{12}(1+2b\tau_p)$	$g_7\ =$	$V^{'}(h)\tau_p - b\tau + \tau b k\tau_p - 2\tau b\beta\tau_r$

$$T = \frac{1}{k_1}T^{'},\ R = \sqrt{\frac{k_1}{k_2}}R' \tag{21}$$

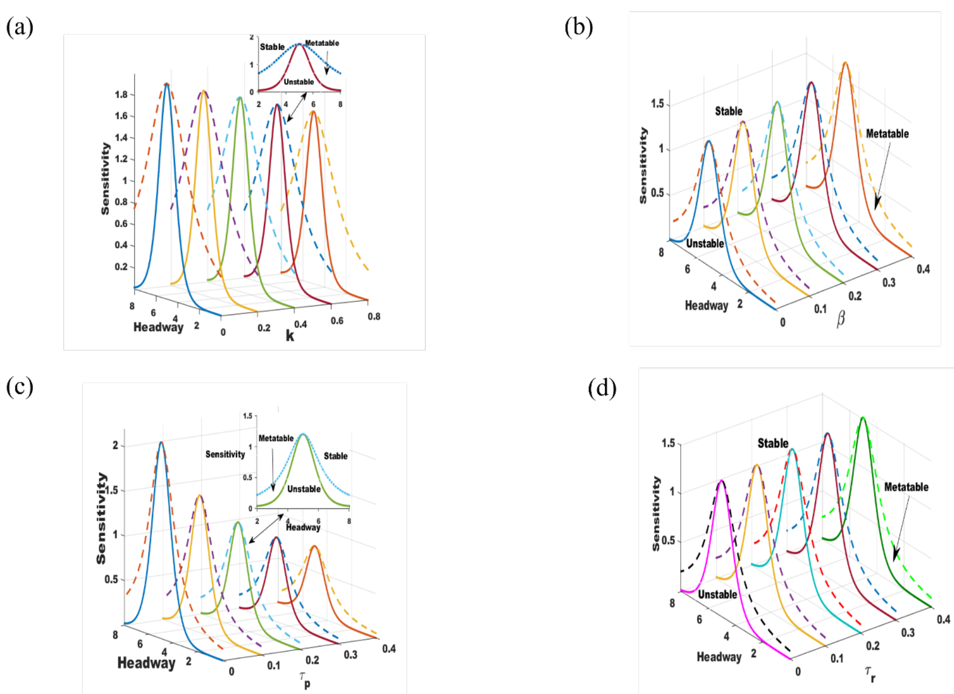

Fig 2. "Phase diagram in parameter space (a)$(\Delta x,\, k,\, \alpha)$ for various values of k and fixed $\tau_r = 0.5,\ \beta = 0.2,\ \tau_p = 0.5$ (b) $(\Delta x,\, \beta,\, \alpha)$ for various values of β and fixed $\tau_r = 0.5,\ k = 0.1,\ \tau_p = 0.2$(c) $(\Delta x,\, \tau_p,\, \alpha)$ for various values of τ_p and fixed $\tau_r = 0.4,\ \beta = 0.2,\ k = 0.2$ (d) $(\Delta x,\, \tau_r,\, \alpha)$ for various values of τ_r and fixed $\tau_p = 0.2,\ \beta = 0.2,\ k = 0.1$"

Therefore, one derives the standard "mKdV equation" with the correction term $O(\varepsilon)$ as below:

$$\partial_T R' - \partial_X^3 R' + \partial_X R'^3 + \varepsilon \overline{M}[R'] = 0 \tag{22}$$

where M
$[R'] = \frac{1}{k_1}(k_3 \partial_X^2 R' + \frac{k_1 k_5}{k_2} \partial_X^2 R'^3 + k_4 \partial_X^4 R')$.
After neglecting the $O(\varepsilon)$ terms, we get "modified KdV equation" whose desired "kink-antikink" solution is

$$R_0^{'}\left(X, T^{'}\right) = \sqrt{c} tanh \sqrt{\frac{c}{2}\left(X - cT^{'}\right)} \tag{23}$$

To determine the propagation speed of the "kink-antikink solution" can be deduced as follows:

$$\left(R_0^{'}, \overline{M}\left[R_0^{'}\right]\right) \equiv \int_{-\infty}^{+\infty} dX R_0^{'} \overline{M}\left[R_0^{'}\right] = 0 \tag{24}$$

Table 2. Values of k_i^s

$k_1 = \frac{(V'(h)(1+3b\tau_p+3b^2\tau_p^2)}{6} - \frac{b^3\tau^2}{6} + \frac{\tau k}{2}(b^3\tau_p^2 + \tau\tau_p b^3 + 2b^2\tau_p) - \frac{\tau\beta b^3}{2}(\tau\tau_r - \tau_r^2)$
$k_2 = -\frac{V'''(h)}{6}$
$k_3 = \frac{b^2\tau_c}{2} - \tau_c k b^2 \tau_p + \tau_c \beta b^2 \tau_r$
$k_4 = -(g_5 + (V^{'}(h)\tau_p - b\tau + \tau bk\tau_p - 2\tau b\beta\tau_r)k_1)$
$k_5 = -(\frac{V^{'''}(h)}{12}(1+2b\tau_p) + (V^{'}(h)\tau_p - b\tau + \tau bk\tau_p - 2\tau b\beta\tau_r)\frac{V^{'''}(h)}{6})$

where $\overline{M}\left[R_0^{'}\right] = \overline{M}[R']$. By integrating Equation (23), the propagation speed c is expressed by

$$c = \frac{5k_2k_3}{2k_2k_4 - 3k_1k_5} \tag{25}$$

Finally, the solution of "mKdV equation" is

$$\Delta x_j(t) = h_c \pm \sqrt{\frac{k_1 c}{k_2}(\frac{\tau}{\tau_c} - 1)} \times [(1 - ck_1)(\frac{\tau}{\tau_c} - 1)t + j] \tag{26}$$

and the amplitude A is

$$\sqrt{\frac{k_1 c}{k_2}\left(\frac{\tau}{\tau_c} - 1\right)} \tag{27}$$

The "Kink-antikink solution" characterizes the coexisting phase of traffic flow as jam and free flow, represented by $\triangle x\ (t) = h_c \pm A$, respectively.Figure 2 shows dotted curves indicating coexisting curves resulting from "nonlinear analyses". Figure 2(**a**) depicts that the neutral stability curve diminishes as k grows from 0.1 to 0.8 when $\tau_r = 0.5$, $\beta = 0.2$ and $\tau_r = 0.5$. Furthermore, we can see from Figure 2(**b**), decrease in the parameter β results in an expansion of the stable zone and a decrease in the amplitude of stability curves and the critical point of curves with fixed $k = 0.1,\ \tau_p = 0.5,\ \tau_r = 0.8$. Moreover, Figure 2(**c**) depicts that the stability increases as the prediction time rises. This implies an expansion of the stability area with an increase in τ_p from 0 to 0.4. This depicts that if we change the predictive time, it helps to enhance the stability. Continuing in this way, Figure 2(**d**) shows the τ_r plays an important role in stabilizing the traffic flow because the unstable region becomes expends as τ_r increases. So, we can conclude that the traffic flow stability increases with a decrease in traffic jerk and an increase in the driver's velocity prediction coefficient. Uncomfortable or dangerous driving situations when abrupt changes in velocity (such as forceful braking or rapid acceleration) take place are associated with high jerk levels. Better navigation systems, roadway management systems, or even algorithms for autonomous vehicles may be designed with the assistance of predictions about when and where these jerks will occur. Driving more smoothly can increase traffic efficiency and safety when velocity is accurately predicted based on the jerk.

3.3 Numerical simulation

The impact of driver's prediction with jerk behavior traffic flow is illustrated in this section using numerical simulations in view of both linear and nonlinear stability analysis. The following periodic boundary conditions are applied to the initial headways as

$$\begin{array}{c}\Delta x_n(0) = \Delta x_n(1) = \Delta x_n(2) = 4.0, (n \neq 50, 51)\\ \Delta x_n(0) = \Delta x_n(1) = \Delta x_n(2) = 4.0 + A,\ (n = 50)\\ \Delta x_n(0) = \Delta x_n(1) = \Delta x_n(2) = 4.0 - A,\ (n = 51)\end{array} \tag{28}$$

Assumed to be on the road are 100 automobiles in total, 400 meters in length, the initial disturbance $A = 0.5,\ v_{max} = 2,\ h = 4$. After 20,000 time steps. Figure 3 displays the "spatiotemporal evolution" of headway with constant $\tau_r = 0.5,\ \tau_p = 0.4,\ \beta = 0.2$ and various values of k ranging from 0 to 0.4, the headway wave in Figure 3 oscillates more and more as the velocity prediction coefficient k progressively falls down. The amplitude of the headway also falls as the velocity prediction coefficient value rises. Stop-and-go traffic arises when a little disturbance breaks the initial flow and gradually travels backward, as seen in Figure 3.Figure 4 shows the simulation results under the prediction time scenario using the fixed variable $\tau_r = 0.4,\ \beta = 0.2,\ a = 3$ and $k = 0.2$ with various values of predictive time τ_p. It demonstrates the development of "stop-and-go" traffic that moves backward after a little disruption to the normal traffic flow. Figure 4 shows that when τ_p grows, the fluctuations get smaller, but when τ_p is sufficiently great (τ_p = 0.4), the fluctuations finally cease to change. Furthermore, we can claim that the amplitude of "stop-and-go" waves fades out when the parameters chosen meet the stability condition (13).

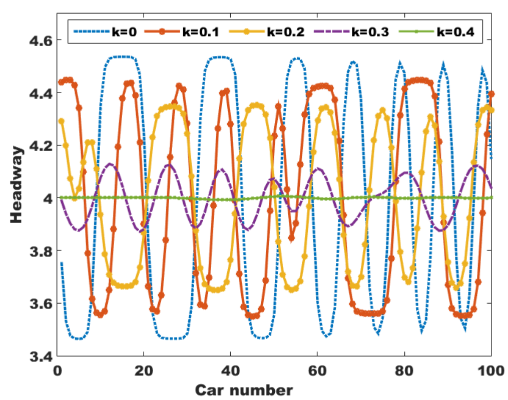

Fig 3. For time t = 20000 − 20300s, the "spatiotemporal headway" shifts when $\tau_p = 0.4,\ \beta = 0.2, \tau_r = 0.5\ and\ \alpha = 3$ for various values of k.

This indicates a state of uniform flow, and traffic flow will continue in a stable state even if a little disruption is going on. We enter the stable zone when the stability criterion for $\tau_p = 0.4$ is met. These results in consistent traffic flow across the region, and the "stop-and-go" waves vanish. Prediction time is therefore essential to minimizing traffic jams and maximizing safety, both of which increase total efficiency. Additionally, the simulations verify that, as the linear and non-linear analysis indicated, well selected prediction parameters can delay or stop the start of instability, resulting in a more stable traffic flow. It shows that after accounting for driving forecasts, traffic flow stability may be improved by the application of "V2X technology". Consequently, the results of the simulation align with the theoretical analysis. In order to forecast vehicle behavior, car-following models and other traffic flow models frequently employ metrics like acceleration and velocity. Jerk is included in the proposed model to provide a more accurate forecast of how velocity changes over time. Low jerk levels, or gentle changes in velocity, are linked to a smoother traffic flow. On the other hand, more chaotic or erratic velocity patterns can be predicted by high jerk levels.

3.4 Discussion

Future transportation is rapidly incorporating "vehicle-to-everything (V2X)" technologies. By enabling communication between automobiles, pedestrians, and roadside infrastructure, this technology makes driving safer and more effective. V2X can aid in easing traffic and enhancing general road safety by offering real-time information on road conditions. A CF model that considers traffic jerks and envisioned future velocities between vehicles in the V2X environment is being created to address

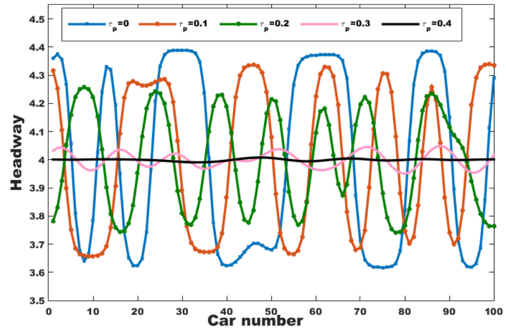

Fig 4. For time t = 20000 − 20300s, the spatiotemporal headway shifts when $\beta = 0.2$, $\tau_r = 0.4$, $k = 0.2$ and $\alpha = 3$ for various values of τ_p.

traffic issues. This model can accurately predict how automobiles will behave in the future, allowing drivers to anticipate their moves and respond accordingly. By enabling drivers to see how far away other cars are from them, the suggested approach improves their ability to predict abrupt changes in speed. In addition to improving road safety, it may also assist drivers save time and energy, making driving more comfortable and pleasurable.

Theoretically, compared to the current models, the suggested model has a smaller area of congestion and greatly increases the range of safe driving circumstances. Furthermore, it is discovered that the suggested model works well for raising the general effectiveness of traffic flow. Figure 1(**a**) displays a headway-sensitivity phase diagrams for comparison of the OVM and the novel model. Equation (13) gives the stability conditions. If k is zero, we may use this equation to forecast jerk, and if β equals zero, it provides stability conditions for estimating the speed of the leading vehicle. Additionally, the OV model[8] satisfies its stability criterion and becomes stable when the k, τ_p, τ_r and β parameters are set to zero.

4 Conclusion

In order to enhance traffic flow stability and lessen crowdedness, this study suggests using a "car-following model" to study the traffic jerk and velocity effect in traffic systems. Traffic congestion is explained by inferring the outcome of the "mKdV equation" and the neutral stability condition. In comparison to the ideal velocity model, the model shows a notable extension of the stable zone in traffic dynamics through both linear and nonlinear stability analysis, especially in the presence of heavy traffic close to crucial locations of congestion. The outcomes of theoretical study indicate that the velocity effect (k) and the coefficient of traffic jerk (β) have a major role in improving traffic flow stability. The theoretical study is supported by the numerical simulation findings, which show that traffic jerk and velocity effect can significantly affect traffic flow stability. Smoother traffic flow and less congestion result from drivers being able to modify their behavior in response to change traffic outputs thanks to the prediction velocity effect term. The model's practical usefulness under periodic boundary conditions is confirmed by numerical simulations, and the resultant "mKdV equation" further identifies important places where congestion is likely to develop. This model might be expanded by investigating how the impacts of driving prediction info on traffic flow with the traffic jerk effect that comes due to the movement of non-motor vehicles in mixed-traffic situations involving both human-driven and autonomous cars. The model might also be used to assess the consequences of different lane-changing behaviors on more intricate road constructions, such as curving roads and multi-lane highways. Furthermore, adding real-time data from connected car technologies might improve the model's precision and usefulness, offering an even greater.

References

1) Wang Z, Shi Y, Tong W, Gu Z, Cheng Q. Car-following models for human-driven vehicles and autonomous vehicles: A systematic review. *Journal of transportation engineering, Part A: Systems*. 2023;149(8). Available from: https://doi.org/10.1061/JTEPBS.TEENG-7836.
2) Yadav S, Redhu P. Self-stabilization control on traffic flow of connected and automated vehicles under cyberattacks. *The European Physical Journal Plus*. 2023;138(12). Available from: https://link.springer.com/article/10.1140/epjp/s13360-023-04791-8.
3) Ren W, Cheng R, Ge H. Bifurcation analysis of a heterogeneous continuum traffic flow model. *Applied Mathematical Modelling*. 2021;94:369–387. Available from: https://doi.org/10.1016/j.apm.2021.01.025.

4) Zhao J, Knoop VL, Wang M. Microscopic traffic modeling inside intersections: interactions between drivers. *Transportation science*. 2023;57(1):135–155. Available from: https://doi.org/10.1287/trsc.2022.1163.
5) Sun L, Jafaripournimchahi A, Kornhauser A, Hu W. A new higher-order viscous continuum traffic flow model considering driver memory in the era of autonomous and connected vehicles. *PhysicaA: Statistical Mechanics and its Applications*. 2020;547. Available from: https://doi.org/10.1016/j.physa.2019.123829.
6) Mehra M, Siwach V, Mehta M, Redhu P. Analyzing psychological information using lattice hydrodynamic model coupled with electronic throttle control. *International Journal of Information Technology*. 2024. Available from: https://link.springer.com/article/10.1007/s41870-024-02020-8.
7) Wang Z, Liu Z, Cheng Q, Gu Z. Integrated self-consistent macro-micro traffic flow modeling and calibration framework based on trajectory data. *Transportation research part C: emerging technologies*. 2024;158. Available from: https://doi.org/10.1016/j.trc.2023.104439.
8) Tan H, Yin C, Peng G. Impact of the visibility effect on phase transitions in lattice hydrodynamic model under the bad weather traffic environment. *Chinese Journal of Physics*. 2024;89:46–55. Available from: https://doi.org/10.1016/j.cjph.2024.01.035.
9) Redhu P, Yadav D, Siwach V. A novel car-following model incorporating advance reaction time with passing. *The European Physical Journal Plus*. 2024;139. Available from: https://link.springer.com/article/10.1140/epjp/s13360-024-05365-y.
10) Yang H, Yu W, Zhang G, Du L. Wide Traffic Flow Dynamics Prediction Leveraging Macroscopic Traffic Flow Model and Deep Neural Networks. *IEEE Transactions on Intelligent Transportation*. 2024;25(5):4443–4457. Available from: https://ieeexplore.ieee.org/document/10399846.
11) Zhao HT, Zhao X, Lu JC, Xin LY. Cellular automata model for Urban Road traffic flow Considering Internet of Vehicles and emergency vehicles. *Journal of Computational Science*. 2020;47. Available from: https://doi.org/10.1016/j.jocs.2020.101221.
12) Feng T, Liu K, Liang C. An improved cellular automata traffic flow model considering driving styles. *Sustainability*. 2023;15(2). Available from: https://doi.org/10.3390/su15020952.
13) Yin YH, Lü X, Jiang R, Jia B, Gao Z. Kinetic analysis and numerical tests of an adaptive car-following model for real-time traffic in ITS. *Physica A: Statistical Mechanics and its Applications*. 2024;635. Available from: https://doi.org/10.1016/j.physa.2024.129494.
14) Peng G, Luo C, Zhao H, Tan H. Phase transitions of dual-lane lattice model incorporating cyber-attacks on lane change involving inflow and outflow under connected vehicles environment. *Chaos, Solitons & Fractals*. 2024;181. Available from: https://doi.org/10.1016/j.chaos.2024.114697.
15) Mehta S, Redhu P. Impact of driver prediction with density deviation and anticipation in lattice hydrodynamic model with passing. *Physica Scripta*. 2024;99. Available from: https://iopscience.iop.org/article/10.1088/1402-4896/ad693f.
16) Yadav S, Siwach V, Redhu P. Impact of driver's advanced reaction time in car-following model with optimal velocity deviation under V2X environment. *Europhysics Letters*. 2023;143. Available from: https://iopscience.iop.org/article/10.1209/0295-5075/acf51d.
17) Redhu P, Siwach V. An extended lattice model accounting for traffic jerk. *Physica A: Statistical Mechanics and its Applications*. 2018;492:1473–1480. Available from: https://doi.org/10.1016/j.physa.2017.11.074.
18) Zhai C, Wu W. Analysis of drivers' characteristics on continuum model with traffic jerk effect. *Physics Letters A*. 2018;382(47):3381–3392. Available from: https://doi.org/10.1016/j.physleta.2018.09.029.
19) Cheng RJ, Ge HX, Wang JF. The nonlinear analysis for a new continuum model considering anticipation and traffic jerk effect. *Applied Mathematics and Computation*. 2018;332:493–505. Available from: https://doi.org/10.1016/j.amc.2018.03.077.
20) Liu Y, Cheng RJ, Lei L, Ge HX. The influence of the non-motor vehicles for the car-following model considering traffic jerk. *Physica A: statistical mechanics and its applications*. 2016;463:376–382. Available from: https://doi.org/10.1016/j.physa.2016.07.042.
21) Jin Z, Li Z, Cheng R, Ge H. Nonlinear density wave investigation for an extended car-following model considering driver's memory and jerk. *Modern Physics Letters B*. 2018;32(01). Available from: https://dx.doi.org/10.1142/s0217984917503663.
22) Yu S, Huang M, Ren J, Shi Z. An improved car-following model considering velocity fluctuation of the immediately ahead car. *Physica A: Statistical Mechanics and its Applications*. 2016;449:1–17. Available from: https://dx.doi.org/10.1016/j.physa.2015.12.040.
23) Yadav S, Redhu P. Impact of driving prediction on headway and velocity in car-following model under V2X environment. *Physica A: Statistical Mechanics and its Applications*. 2024;635. Available from: https://dx.doi.org/10.1016/j.physa.2024.129493.
24) Yadav S. Impact of visibility on car-following considering traffic jerk in adverse weather conditions. *The European Physical Journal Plus*. 2024;139. Available from: https://dx.doi.org/10.1140/epjp/s13360-024-05334-5.